Toward Crowdsourcing-Based Road Pavement Monitoring by Mobile Sensing Technologies

Chih-Wei Yi, *Member, IEEE*, Yi-Ta Chuang, and Chia-Sheng Nian

***Abstract*—In crowdsourcing applications, the quality of the crowdsourced data is decisive to the success of subsequent system-level mining processes. We proposed a smartphone probe car (SPC) system to monitor road pavement. An SPC is essentially an ordinary vehicle with a mounted smartphone that runs sensing programs to objectively assess bumping caused by road anomalies such as potholes and bumps. The proposed system has several features. First, to allow dynamic forming of SPCs, we develop a signal processing heuristic for the extraction of the vertical acceleration components from the accelerometer readings (upon which bumping detection and road surface anomaly assessment rely). By these means, the proposed system provides a driver-friendly environment, requiring neither complicated installation nor driver-assisted training processes, and thus is possible to achieve hassle-free mass deployment such that drivers would be willing to participate in crowdsourcing. Second, based on the underdamped oscillation model, we propose a road anomaly indexing heuristic that is representable for road anomalies rather than vehicle conditions. This will later facilitate the system-level data mining processes in the servers. Third, a prototype SPC system was implemented and extensive field tests were undertaken to verify the performance of our system framework. Furthermore, we experimentally adopted a DENCLUE-like algorithm to mine road anomaly information from reported events to demonstrate any potential benefit from future investigation of data mining process at the system level. We believe the research works introduced in this paper consist the first step toward building an "ecosystem" of SPC-based crowdsourcing traffic and road monitoring applications.**

***Index Terms*—Crowdsourcing, mobile sensing, road pavement monitor, smartphone probe car (SPC).**

I. Introduction

ROAD networks connecting buildings, villages, cities, and even countries are the most important transportation infrastructure in modern life. The surface condition of sealed roads is directly related not only to driving experience and traveling comfort, but more importantly to driving safety. For a responsible government, it is important to maintain the good condition of road networks. Awareness of road surface anomalies in the earliest manner possible is the first step toward prompt repair. By cooperating with mobile sensing technologies, it is possible to develop a vehicle-based crowdsourcing system that automatically and pervasively monitors the existence of road surface anomalies. In this paper, we develop a smartphone probe car (SPC) system based on mobile sensing technologies to detect and assess road surface anomalies such as potholes and bumps.

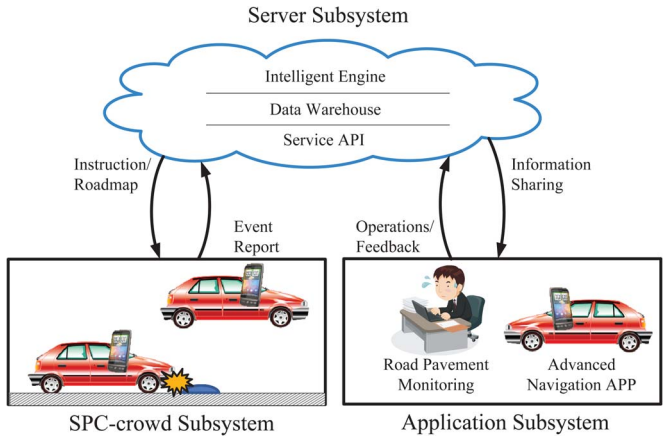

Fig. 1. SPC-based crowdsourcing system framework.

An SPC is an ordinary vehicle equipped with a mounted smartphone that executes sensing programs to detect significant bumping, most likely caused by the vehicle running over road anomalies. SPCs report detected bumping events to cloud servers either via an online wireless connection or by uploading log files in a batch. As illustrated in Fig. 1, in our framework, there are two subsystems in addition to the SPC crowd subsystem: the server subsystem and the application subsystem. The server subsystem provides service application programming interfaces (APIs) for collecting data from the SPC crowd and for sharing information with applications, data mining engines for extracting road anomaly information from crowdsourced data, and data warehouse capabilities. By utilizing the road anomaly information, the application subsystem can provide various advanced services. In some services, such as advanced navigation, the application subsystem can be integrated with the SPC software such that the proposed framework can then form a self-contained supply-and-demand ecosystem. For such a system to be possible, first of all, the SPCs need to be able to

Manuscript received December 16, 2013; revised June 21, 2014 and October 24, 2014; accepted December 2, 2014. Date of publication March 9, 2015; date of current version July 31, 2015. The work of C.-W. Yi was supported in part by Sinica under Grant AS-102-TP-A06; by the Ministry of Science and Technology under Grant NSC101-2628-E-009-014-MY3, Grant NSC102-2918-I-009-002, Grant MOST 103-2218-E-009-010, and Grant MOST 103-2218-E-009-021; by the Ministry of Education Aim for the Top University Plan; and by NCTU and ITRI Joint Research Center. The Associate Editor for this paper was Dr. J. V. Krogmeier. *(Corresponding author: Chih-Wei Yi.)*

C.-W. Yi and Y.-T. Chuang are with the Department of Computer Science, National Chiao Tung University, Hsinchu 30010, Taiwan (e-mail: yi@cs.nctu.edu.tw).

C.-S. Nian is with HTC Corporation, Taipei 231, Taiwan.

Color versions of one or more of the figures in this paper are available online at http://ieeexplore.ieee.org.

Digital Object Identifier 10.1109/TITS.2014.2378511

be massively deployed in a convenient and hassle-free manner; second, the crowdsourced data need to preserve consistency across its assessments of road anomalies.

In the literature, various mobile sensing technologies have been proposed to detect road anomalies (such as potholes, uneven manhole covers, and speed bumps) or to assess road surface conditions. One of the most popular approaches is to detect the vibrations of vehicles as they run over anomalies. In most studies, accelerometers, usually called G-sensors, were used to measure the vibrations, and GPS receivers, simply called GPS for short, were used to obtain the speed and location of the vehicles [1]–[8] Some researches have also suggested utilizing the noise level recorded by microphones as references [1], [9]. Other research works adopted a stereo-vision-based technique to detect the road anomalies [10], [11]. However, they primarily focused purely on the detection and only seldom discussed their assessments. The majority of sensing technologies developed in previous works require either a complicated installation or the provision of training. This problem becomes more significant if crowdsourcing approaches are adopted since vehicles, mobile devices, and mounting methods may be different across cases, which hinders those technologies from mass deployment.

In this paper, we propose a solution that has the potential for pervasive deployment. First, since the proposed sensing algorithm detects bumping events based on the vertical components (VCs) of acceleration, we introduce a signal processing technique to extract the VCs from the G-sensor readings with the result that drivers do not need to install smartphones. Second, taking the underdamped oscillation model (UOM) as the basis, we develop an anomaly index (AI) heuristic to objectively grade road anomalies. In the assessment system, in addition to vehicle speed, the physical properties of the complex coupling of the vehicle–smartphone system with auxiliary mounting devices are taken into consideration. In short, the proposed AI can provide superior cross-SPC consistency in the assessment of road anomalies. In addition, the proposed solution is adaptive, and no training processes are required. Finally, the proposed algorithm does not have strict hardware specifications and can be easily transplanted to most smartphones. Note that the sampling rate of the G-sensor must be 20 Hz to detect bumping events, as reported by [6]. Due to advancements in microelectronic mechanical system technology, most smartphones sold today meet this requirement. Considering all of these advantages, the proposed SPC system provides a solid foundation for the development of a crowdsroucing-based road pavement monitoring system.

The reported events are composed of three pieces of information: the timestamp, the position, and the AI of the detected road anomalies. Although we have provided an assessment system of run-over anomalies, other issues must still be considered. For example, it is possible that SPCs may not run over anomalies even when they pass over road segments where the anomalies actually exist, and it should be noted that GPS data cannot be relied upon to be perfectly accurate. The existence of road anomalies is not completely stable but may differ from time to time due to repair and the effects of harsh weather. It is also possible that the event detection algorithm could fail. Therefore, system-level intelligence must be provided in order to extract information from crowdsourced data. To demonstrate the possibility of developing a road pavement monitoring system, we apply a DENCLUE-like clustering algorithm to mine road anomaly information from reported events. The results of two data sets will be provided later in this paper.[1]

In this paper, we propose an adaptive SPC system for developing crowdsroucing-based road pavement monitoring systems, which is the key to pervasive deployment and highly referenced crowdsourced data. The formation of SPCs is simple, requiring no complicated installation and no training. The proposed AI can provide a cross-SPC assessment of road anomalies. A prototype system was implemented, and extensive road tests were executed to collect data. A DENCLUE-like clustering algorithm was provided to extract information about road anomalies to validate the proposed framework.

The rest of this paper is organized as follows. Section II reviews the relevant literature; Section III introduces the proposed system architecture and the challenges involved in its development; in Section IV, a device-level feature extraction heuristic is proposed that extracts vertical components (VCs) and SPC-level parameters; Section V presents a grading algorithm for road surface anomalies based on the UOM; in Section VI, a DENCLUE-like clustering algorithm is applied to filter out noise and improve the location accuracy of anomalies, and some experimental results are provided to validate the proposed system, and Section VII presents our conclusion and discusses possible future works.

II. Related Work

The quality of roads is one of the most observable metrics to evaluate the performance of governments. Governments are hence willing to annually allocate a large portion of budget in construction and maintenances of road infrastructures to improve their reputation to citizens. For example, Taipei City Government has been launching a multiple-year project [12] to improve the quality of roads by removing bumps and potholes. The main tasks include the following: 1) improving the robustness of roadbeds; 2) covering manholes to increase the smoothness of roads; 3) routines of road inspections and pothole repairs; and 4) on-demand maintenances. The government has allocated a budget of 2 billion NT dollars (around 66 million U.S. dollars) in 2009 and 2.58 billion NT dollars (around 86 million U.S. dollars) in 2010 for this project. Although the project has been ongoing for several years, citizens still have critics about the efficiency and even effectiveness of this project. Furthermore, the city government must dedicate commissioners to inspect road conditions in different areas every day, which results in high demand for human resources in order to achieve real-time inspections.

To avoid high human resource demands, many works based on probe car systems were proposed for environmental sensing [1]–[7]. BusNet [1], which is a bus-based probe car system, was proposed to monitor road and environmental conditions along

[1]Due to space limitations, the experimental results performed in the Xin-an Road scenario were skipped. Please refer to the supplementary materials for details.

bus routes. A Crossbow MICAz mote [1] equipped with several sensor boards, including a GPS receiver, a triaxial accelerometer, a thermometer, and a carbon monoxide sensor, was installed on each bus. The vibrations measured by the accelerometer are the preliminary observation of anomaly detection.

In contrast to probing along fixed bus routes, Pothole Patrol [2], a taxi-based mobile sensing system, was proposed for pervasive road surface monitoring. A taxi probe car was equipped with sensors, including an accelerometer, a GPS receiver, and a notebook being the data sink and processing unit. The system adopted a client–server architecture. For the client side, anomaly events are detected by a multithreshold algorithm based on the moving speeds, frequency of vibrations, peak vertical vibrations, ratio of horizontal to vertical vibrations, and ratio of vertical vibrations to speeds. For the server side, after anomaly events are collected from probe cars, a distance-based clustering algorithm is utilized to filter out noise based on the cluster size and to improve positioning accuracy. However, in this paper, sensors can be only installed either at the dashboard or on the windshield. The clustering algorithm is merely used to filter errors in detection and positioning of anomaly events without further investigation, such as the hitting ratio of road anomalies that is the ratio of the number of reported events to the number of passing probe vehicles. The hitting ratio may implicitly distinguish the dimension of road anomalies. Even more, sensors must be carefully aligned with vehicles, which restricts the practice of this system. In addition, how to determine the thresholds used in the anomaly detection algorithm is not addressed.

In [6], a vehicle probe-based pavement maintenance project was proposed. A probe car was required to be equipped with accelerometer and GPS and capable to be operated with dedicated short range communications (DSRCs). Probe data were collected via DSRCs and processed and analyzed in the data processing center offline. Both root mean square of vertical accelerations and suspension energy were used to estimate the International Roughness Index (IRI) [13], which is used in the assessment of pavement quality. For pothole detection, a threshold-based and a wavelet transform algorithm were proposed based on vertical accelerations.

In [8], a recursive signal processing approach based on correlation averaging was proposed to jointly filter noise from probe vehicles. The noise comes from two sources, namely, additive errors from accelerometers and data registration errors from GPS, driving path variation and onboard distance-measuring devices. However, the vehicle dynamics that may affect the vibration measurement is not covered.

Smart handheld devices with embedded sensors were used in Nericell [3]. To allow the handheld device being flexibly installed on vehicles and resolve the alignment issue and various road geometries, e.g., curve roads, a heuristic was proposed to automatically find out the Euler matrix between handheld devices and vehicles. The anomaly detection algorithm is still threshold based. To deal with different driving speeds, two sets of thresholds were used for the vehicle moving at a high ($\geq$ 25 km/h) and a low ($<$ 25 km/h) speed, respectively. However, how to determine thresholds is still mysterious in most threshold-based works. Street Bump [7], a crowdsourcing project that adopts smartphones, was launched. Volunteers use the Street Bump mobile application to collect road condition data while driving and report possible potholes to governments to repair them and as references in long-term pavement maintenance. In [4], a machine-learning-based road anomaly detection method, which adopts smartphones as sensors, was proposed for motorcycles. The IRI was redefined to the number of road anomalies on roads per distance. Both supervised and unsupervised learning approaches were studied. For the supervised learning approach, a relabeling mechanism for training data was proposed. For the unsupervised learning approach, a clustering-based method was proposed to obtain thresholds for road anomaly detection. No matter if it is supervised or unsupervised learning method, both need large amounts of data to train their detection models.

More threshold-based methods for road anomaly detection were proposed in [5], including the Z-THRESH method, which detects by a vertical vibration, the Z-DIFF method, which detects by the difference of consecutive VCs of acceleration, the STDEV(Z) method, which determines by the standard deviation of VCs of acceleration in a window, and the G-ZERO method, which detects whether the sensor senses a 0-G vibration. A heuristic to determine the thresholds was proposed based on true positive and false positive of the detection rate. However, how to determine the threshold is not trivial. In particular, for different devices and different mounting methods, it needs to retrain their system parameters every time.

In summary, to be part of a crowdsourcing system, the SPC should possess several capabilities such that users can easily use the detection software installed in the smartphone. For example, the SPC should be able to overcome the alignment issue caused by the posture of a smartphone such that users do not need to worry about the installation of smartphones; the road quality assessment should be cross-SPC, i.e., the assessment results of an anomaly reported by different SPCs should possess similarity.

III. Proposed System and Main Contributions

Here, we sketch the proposed road pavement monitoring system and then turn our focus on the technical challenges involved in developing the SPC system.

A. System Architecture

Based on the framework introduced in Section I, we design a prototype system to monitor road pavement. As illustrated in Fig. 2, the proposed system is composed of three parts: the SPC application bundled with advanced services, the Cloud Server, and the Road Pavement Management System.

An SPC is a mobile sensing system formed by a vehicle dynamically coupling with a mounted smartphone running the SPC application. The GPS can provide the speed and location of the SPC, and the G-sensor can measure the vibrations. Based on the sensing data, the intelligent sensing (Int. Sensing) module detects and assesses run-over road anomalies. The intelligent sensing module should be adaptive to vehicle conditions, smartphone specifications, and installation postures. The wireless

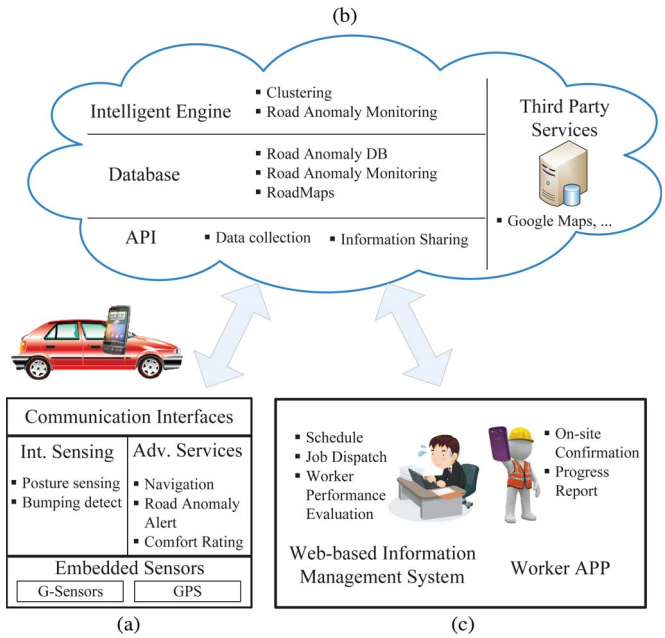

Fig. 2. Proposed road pavement monitoring system.

communication interfaces of smartphones, e.g., WiFi and 3G, are used to report events to or obtain information or instructions from the cloud servers. Events can be reported by either online or batch uploading. The advanced services (Adv. Services) module provides attractive services such as navigation, road anomaly alert, and comfortableness rating so that drivers are willing to use the application and participate in data collection, which is a key to the success of a crowdsourcing ecosystem.

The cloud servers are the centerpiece of the system. Service APIs are implemented for SPCs to report bumping data and for applications to acquire traffic and road information. The cloud servers also need to provide database services to store bumping data and road anomaly information. The intelligent engine provides for data mining capability to extract information from reported bumping data and autonomous monitoring capability on road pavement. In addition, third-party services, e.g., Google Maps [14], are used to develop user interfaces and obtain digital maps and navigation information.

The road pavement management system provides for continuous road pavement monitoring and maintenance. It contains a web-based information management system and a worker application. The web-based information management system is used for road pavement managers to schedule and dispatch maintenance jobs and evaluate the performance of workers; the worker application is used to facilitate the road pavement repairs such as on-site confirmations and progress reports.

B. Challenges and Strategies

In this paper, we focus on developing the SPC-level intelligent sensing capabilities and demonstrating possible benefits from the system-level intelligence. The rest of the proposed system will be left to our next work. In the following, we outline the technical challenges involved in developing the system and the corresponding strategies to cope with these challenges.

As mentioned earlier, an SPC is a dynamic coupling of a vehicle and a mounted smartphone. To promote the solution, the most important thing is that the forming of SPCs and the operation of the SPC application should be as simple as possible and without bringing any issues to the drivers. Furthermore, the detection and indexing algorithms should preserve cross-SPC consistency. In other words, even detected by different SPCs, the reports of bumping events due to the same road anomalies should be similar. The results should not be significantly affected by other non-road-anomaly factors such as smartphone models, mounting methods, and the conditions and running speeds of vehicles. The SPC-level intelligence [8] should be self-adaptive to the environment context to provide the following capabilities.

- Posture awareness: The mounted posture of smartphones affects the orientation of the sensor frame and thus the g-vectors. Since the responsibility of drivers is only to mount the smartphones and run the application, the SPC system itself should be aware of the smartphone posture and have the capability to extract preferred features for anomaly detection.
- Self-learning capability: The system should have the capability to learn the system parameters for road anomaly detection and indexing without user-involved training. Otherwise, it would discourage users from participating in the crowdsourcing process.
- Cross-SPC assessment: Under different conditions, e.g., SPC association and vehicle speeds, the system should provide similar results for the same anomalies, not only the detection of road anomalies but also the assessment of road anomalies.
- Robust to the specification of smartphones: Smartphones of different models may have various sampling rates. In addition, the sampling frequency may be affected by central processing unit loading. Hence, the proposed methods should be tolerant of some levels of inaccuracy in the sampling frequency.
- Data usage: In a crowdsourcing system, the data source is contributed by the crowds. Since the communication interface for the vehicle traffic is mainly via mobile networks such as 3G/LTE, the data usage will be considerable if excessive unnecessary data are reported, which may discourage the user to contribute in the crowdsourcing process. Therefore, it is important to extract key features that represent the severity of road anomalies.
- Power consumption: Since the smartphone battery is the most valuable resource to keep applications alive, the running detection should be less power consumed. To investigate the components of energy consumption and the amount of power consumed in our methods, we use a power monitor tool to measure the average currents of the padfone model for 1 min under eight different levels. We consider the components of power consumption, including the operating system (OS), the screen, the user interface (UI) refreshing, the map application (map app), the mobile network interface (NIC), the sensor operating in normal mode (20 Hz) or fastest mode (40 Hz), and our detection application (detection app). Note that, since the

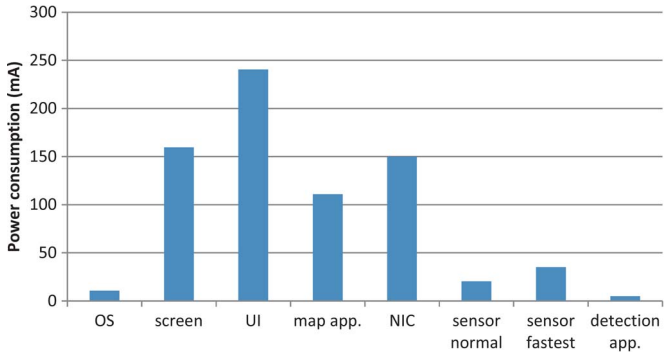

Fig. 3. Components of power consumption measured in milliamperes. The components of power consumption include the OS, the screen, the UI refreshing, the map application, the network interface, the sensor operating in normal or fastest modes, and our detection application.

detection application uses the GPS to locate the location of a bumping event and the accelerometer to detect the bumping event, they are the main components to consume the battery energy. The results are shown in Fig. 3. It can be noted that the top three power consumed components are the screen, the UI, and the NIC; and the sensor operation mode is relatively less power consumed.

To address these requirements, we develop the following solutions corresponding to these challenges.

- Statistics approach: The proposed algorithms rely on statistics on sensor readings in a period of time instead of an individual. Therefore, the assessment would be more objective and not significantly affected by unstable sampling rates.
- VC extraction: A feature extraction heuristic is introduced to extract the VCs of g-vectors upon which the bumping detection algorithm relies. Since the geometric relation of the SPC coupling is implicitly learned, drivers do not need to get involved.
- UOM: The vibrations of onboard devices are modeled as underdamped oscillation systems. Based on this model, the vibration characteristics of SPCs will be represented by a long-term standard deviation. Again, drivers do not need to get involved.
- AI: Based on the UOM, an assessment metric called anomaly index will be introduced. In short, this index is the ratio of a short-term standard deviation to a long-term standard deviation of the VCs of g-vectors.
- Grouping by the vehicle speeds: The running speeds of vehicles are an important factor that affects the vibrations of vehicles. Since there are no simple models to describe the relation between them, the statistics works will be divided into several categories according to vehicle speeds such that the impacts could be minimized.

Although the proposed SPC system provides the possibility of being transplanted on various smartphones and facilitates the formation of SPCs, the SPC-level intelligence is not enough to build the road pavement monitoring system. For example, if vehicles do not run over the road anomalies, there will be no events at all; even if vehicles run over a road anomaly, the reports for the same road anomalies may have different location information due to the inaccuracy of GPS; although we spent lots of efforts to develop objective assessment, we still cannot get exactly the same AI for the same road anomalies. System-level mining capabilities are necessary to fuse the assessment results from the crowdsourced data and extract sophisticated information. However, since this is not the major task of this paper, we only design a DENCLUE-like clustering algorithm to process the crowdsourced data and extract the information of road anomalies. Experimental results from two data sets will be provided and discussed in Section VI.

IV. SPC-Level Feature Extraction

The proposed intelligent sensing module needs the VCs of g-vectors to detect the anomaly events and index the road anomalies. However, since SPCs are dynamic pairing, the orientations of the smartphones are different from one SPC to another. Here, we propose a VC extraction heuristic (VCEH) to extract VCs. The main task here is to estimate the gravity vector in the sensor frame. After that, VCs can be given by the scalar projection of g-vectors onto the gravity vector. In the meantime, a long-term standard deviation of VCs will be calculated as the parameter to model the vibration characteristics of the SPC system.

A. VC Extraction

We observe that the gravity is the major component of the g-vectors at most times. Therefore, in case the smartphone is mounted on the rack, by applying principal component analysis (PCA) on a collection of g-vectors, we can find the direction of the gravity. For the sake of calculation simplicity and power saving, instead of applying complicated PCA, we adopt running average to find the gravity vector. In addition, to improve the accuracy, g-vectors significantly contaminated by acceleration will be omitted from the running average process.

Let $\overline{\mathbf{g}}_t$ denote the running average of the g-vector by time t over a time period T_1. The calculation of $\overline{\mathbf{g}}_t$ can be expressed as

$$\overline{\mathbf{g}}_t = \operatorname*{avg}_{(t-T_1\le s<t)\wedge\left(\left\|\mathbf{g}_s-\overline{\mathbf{g}}_{t^-}\right\|\le\delta\right)} \mathbf{g}_s \tag{1}$$

where δ is a stable threshold to filter out contaminated g-vectors that are significantly different from the previous running average. Fig. 4 shows the cumulative density function (CDF) of $|\Delta g_v| = |\|\mathbf{g}_s - \overline{\mathbf{g}}_{t^-}\||$ obtained from a field test. Since the purpose of δ is to find out significant vibrations and to reduce unnecessary amount of computation, we choose the 95th percentile of $|\Delta g_v|$ (2 m/s^2) as δ, which captures 5% of significant vibrations while reducing 95% computation at the same time. Let $g_t^{\perp}$ denote the VC of the g-vector at time t. Then, we have

$$g_t^{\perp} = \langle \mathbf{g}_t, \overline{\mathbf{g}}_t \rangle / \|\overline{\mathbf{g}}_t\| \tag{2}$$

where $\langle \mathbf{u}, \mathbf{v} \rangle$ denotes the inner product of the two vectors, and $\|\cdot\| = \langle \cdot, \cdot \rangle^{1/2}$ denotes the norm notation.

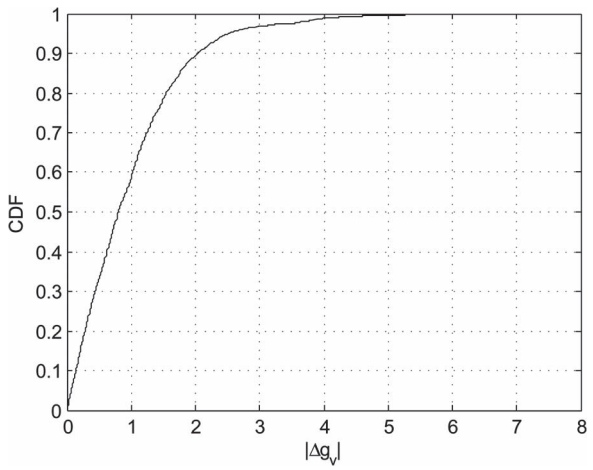

Fig. 4. CDF of $|\Delta g_v| = |\|\mathbf{g}_s - \overline{\mathbf{g}}_{t^-}\||$ obtained in a field test. The field test was performed in the National Chiao Tung University (NCTU) campus, Taiwan, on September 11, 2014. A Ford Windstar 2003 model was used with a zenfone model mounted on a rack and attached to the windshield to collect the data.

B. Validation of Concept

Experiments were executed to validate the proposed concept of VC extraction. In the first experiment, a Sony Xperia S smartphone with a sampling rate 80 Hz was attached to the dashboard of a vehicle with its z-axis aligned to the direction of the gravity as the vehicle parking on a horizontal plane. About 30 min of data were logged as the vehicle drove on a highway. The gravity vector was estimated by a batch approach or an online approach. In the batch mode, the gravity is obtained by taking average on g-vectors over all stable periods, whereas in the online mode, the gravity is estimated by taking average over the stable periods in the last minute. A 1-s period is called stable if the magnitude of every g-vector in this period is less than the stable threshold (δ). A piece of 80-s data as the vehicle runs on a horizontal road segment is illustrated in Fig. 5. In this time-acceleration figure, plots from top to bottom show the z-component of the sensor readings and the VCs calculated by the batch mode and by the online mode, respectively. The z-component is considered as the ground truth. We can see that the three waveforms are almost perfectly aligned. For example, the crests marked by the vertical dash line are with coordinates (18 ms, 11 m/s^2) in these three plots. Numerically, compared with the z-component, the RMSEs are 0.01 m/s^2 of the batch mode and 0.03 m/s^2 of the online mode.

To implement the online version, it is not sure whether the 60-s running average window size is appropriate. Hence, we performed another experiment in which two hTC Desire smartphones with a sampling rate 48 Hz and one hTC Hero smartphone with a sampling rate 46 Hz were used. The mounting method of hTC Desire was that it was installed on a rack, and the other two were attached to the windshield. Various running average window sizes from 10 to 90 s were tested. Since the ground truth was unknown in this experiment, the gravity estimated by the batch mode was taken as the baseline. The results show that the window size 60 s will suffice to achieve the RMSE around 0.02 m/s^2 for the three different mounted methods. In the following analysis, the window size will be denoted by T_1 and set to 180 s.

C. VCEH

To reduce the computation load to the smartphone, the introduced idea will be adapted such that most parameters are updated per second. Before giving the algorithm, we introduce some notations.

- T_0 is the time for system initiation, which is set to 1 min in our experiments.
- T_1 is the running average window size, which is set to 3 min in our experiments.
- G_i is the collection of the g-vectors in the ith second.
- $\overline{\mathbf{g}}_i$ is the estimated gravity vector at the end of the ith second.
- $G_i^{\perp}$ is the collection of the VCs of the g-vectors in the ith second, i.e.,

$$G_i^{\perp} = \left[g^{\perp} \,\middle|\, g^{\perp} = \frac{\langle \mathbf{g}, \overline{\mathbf{g}}_{i-1} \rangle}{\|\overline{\mathbf{g}}_{i-1}\|} \text{ for all } \mathbf{g} \text{ in } G_i \right]. \quad (3)$$

- S denotes the set of indices of stable periods within the running average window.
- σ_i denotes the standard deviation of the VCs in stable periods at the end of the ith second.

The input of the algorithm is V_i for $i = 1, 2, \ldots$, and the outputs of the algorithm is $\overline{\mathbf{g}}_i$ and $G_i^{\perp}$ for $i = 1, 2, \ldots$. Based on the given notations and discussion, the algorithm is given in Algorithm 1.

ALGORITHM 1 Vertical Component Extraction Heuristics

1: // assume the smartphone has been mounted on the rack.
2: $T_0 = 30$; $T_1 = 180$;
3: **INIT**:
4: Initialize all parameters.
5: **repeat**
6: wait for 1 s and read G_i
7: $i = i + 1$
8: $G_i^{\perp} = [g^{\perp} \mid g^{\perp} = \langle \mathbf{g}, \overline{\mathbf{g}}_{i-1} \rangle / \|\overline{\mathbf{g}}_{i-1}\|$ for all $\mathbf{g}$ in $G_i]$
9: **if** $|g^{\perp} - \|\overline{\mathbf{g}}_{i-1}\|| < \delta$ for all $g^{\perp}$ in $G_i^{\perp}$ **then**
10: $S = S \cup \{i\}$
11: **end if**
12: **if** $i > T_1$ **then**
13: $S = S - \{i - T_1\}$
14: **end if**
15: **if** $|S| < T_0/3$ **then**
16: GOTO INIT
17: **end if**
18: $\overline{\mathbf{g}}_i = \underset{\mathbf{g} \text{ is in } G_j \text{ for } j \in S}{\text{avg}} \mathbf{g}$; $\sigma_i = \underset{g^{\perp} \text{ is in } G_j^{\perp} \text{ for } j \in S}{\text{stdev}} g^{\perp}$
19: **until** the program is terminated

At the stage of initialization, the program waits T_0 seconds to read $G_1, G_1, \ldots, G_{T_0}$ and then initializes variables as follows. $S = \{1, 2, \ldots, T_0\}$; $\overline{\mathbf{g}}_i$, for $i = 0, 1, \ldots, T_0$, is set to the average of all g-vectors in the first T_0 seconds; $G_i^{\perp}$, for $i = 1, 2, \ldots, T_0$, is calculated according to (3); σ_i, for $i = 0, 1, 2, \ldots, T_0$, is set to the standard deviation of all entries in $G_1^{\perp}, G_2^{\perp}, \ldots, G_{T_0}^{\perp}$; and at the end, i is given the value T_0. After initialization, the

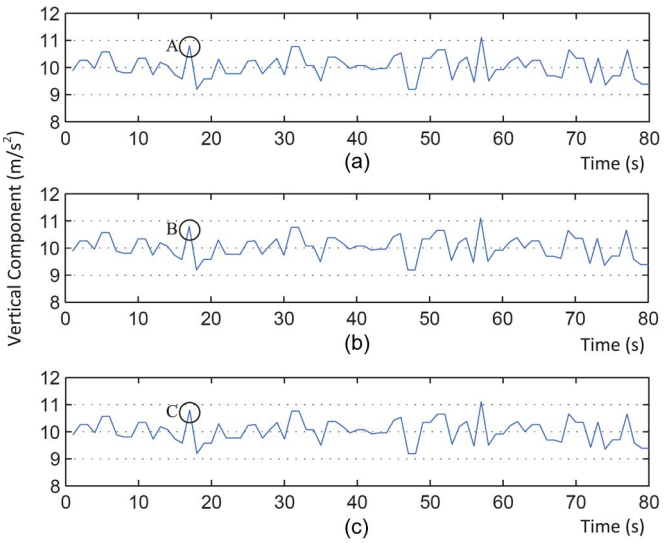

Fig. 5. Waveforms of the (a) z-components of g-vectors and the VCs based on the gravity vectors calculated by the (b) batch mode and the (c) online mode, respectively.

loop between Line 4 and Line 19 will be executed every second until the termination of the program. The codes from Line 15 to Line 17 are an error checking in case the device is not in a stable state. In our implementation, δ is set to 2. $\overline{\mathbf{g}}_i$ and σ_i are updated at Line 18. Note that σ_i, the standard deviation of VCs in stable periods, is a parameter to characterize the oscillation property of the SPC system. It will be utilized in the indexing process in the next section.

V. Road Surface Anomaly Indexing

Here, an indexing algorithm for road anomalies is developed. The algorithm is adaptive to vehicle dynamics, such as vehicle speeds and conditions, without the need of user-assisted training. The input of the indexing algorithm is from the GPS and VCEH. For each detected road anomaly, an index of the anomaly and the time and location information and related statistic parameters will be reported. The main objective of this section is not only detecting but also indexing the road anomalies. Two most important factors, including the SPC system itself and the running speed, are investigated. A solution is provided by modeling SPCs as underdamped oscillation systems. Below, a bumping event detection algorithm is presented first. Then, the underdamped oscillation system is used to model SPCs followed by grouping system parameters by vehicle speeds to mitigate the effects by vehicle speeds. After that, the indexing algorithm of road anomalies is presented.

A. Bumping Events Detection

A typical waveform of VCs as vehicles drove over a bump is illustrated in Fig. 6. The waveform was based on data collected in a Toyota Camry 2013 by a 3DM-GX3-25 accelerometer installed on a rack with a sampling rate of 100 Hz. The SPC run over the bump at a speed of 20 km/hr. The waveform can be divided into two parts: the front wave, in the period from 0.22 to 0.4 s, due to the front wheels running over the bump and the

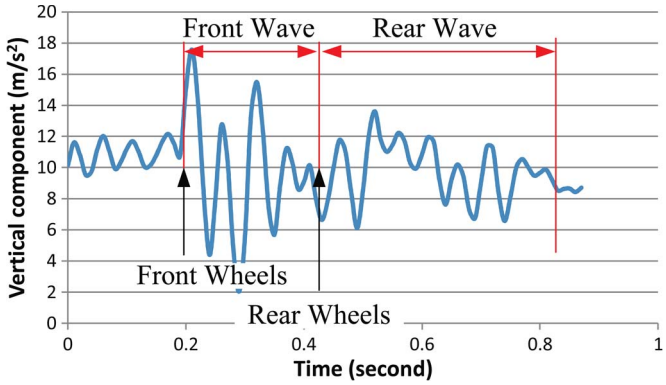

Fig. 6. Waveform of vibrations as a vehicle passes a speed bump at a speed of 20 km/hr. The vehicle model is Toyota Camry 2013, and the speed bump is 3.5 cm high.

rear wave, and in the period from 0.4 to 0.8 s, due to the rear wheels running over the bump. The duration of the front wave can be considered as the time between the front wheels hitting the bump to the rear wheels hitting the bump. The duration of the front wave can be estimated by the distance between two wheel axes divided by the speed.

The bumping events can be detected by recognizing and analyzing abnormal vibrations. We first scan a high pulse in the waveform as the evidence and then analyze the following waveform to confirm or deny the observation. However, the forming of SPCs is dynamic; thus, the characteristics of measured vibrations, e.g., magnitude and frequency, are different from one SPC to another. We need an adaptive threshold to detect the high pulse of the waveform. Recall that, in VCEH, we observe that σ_i could be a parameter representing the oscillation system. A multiple of σ_i could be used as the threshold to detect the high pulse that may imply a bumping event. The bumping event detection algorithm is sketched in the following.

1) For each VC in $V_i^{\perp}$, check whether the difference of the VC and $\overline{\mathbf{g}}_{i-1}$ is greater than $C_1\sigma_{i-1}$, where C_1 is a constant. In our implementation, C_1 is set to 2.
2) If step 1 is satisfied, a potential bumping event is detected and the timestamp recorded and denoted by t_e. Then, the VC series is scanned backward from the time $t_e + \Delta T$ to find when the maximal amplitude in the time interval $[t_e \le j < t_e + \Delta T)$. In our implementation, $\Delta T = 0.5$ was applied. Let $\sigma_{\text{event}} = \mathbf{stdev}_{t_e \le t < t_e + \Delta t} g_t^{\perp}$ be the standard deviation of the VCs in the bumping event.
3) If σ_{event} is greater than $C_2\sigma_{i-1}$, where C_2 is a constant, a bumping event is detected and reported. In our implementation, C_2 is set to 2.5.

Here, we add a remark on the selection of the model parameters C_1 and C_2. Since this work adopts a model-based method (refer to Section V-B) to detect bumping events, it should be noted that the parameters C_1 and C_2 only need to be determined once. Figs. 7 and 8 illustrate the selection of C_1 and C_2 for different SPC settings, respectively. It can be noted that, for different SPCs, the parameters are all similar ($C_1 = 2$, and $C_2 = 2.5$).

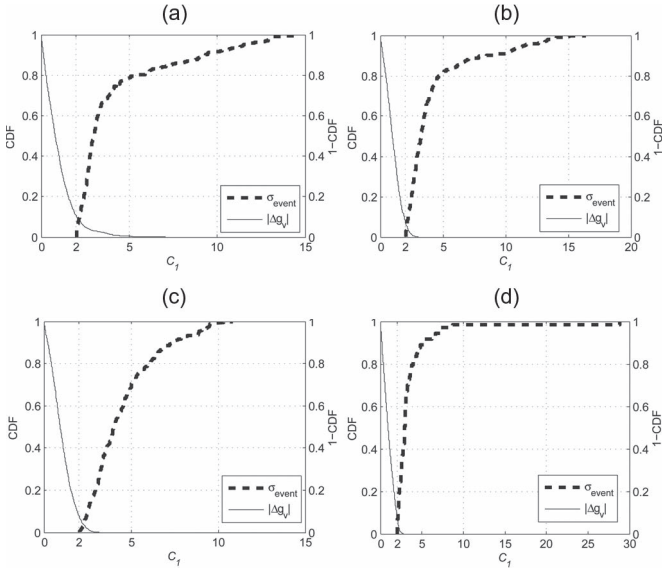

Fig. 7. Illustration of the selection of C_1. For each subplot, the dot line denotes the CDF of σ_{event}, and the solid line denotes the 1-CDF (survival function) of $|\Delta g_v|$. The field test was performed in the NCTU campus, Taiwan, on September 11, 2014. Two vehicles (Ford Windstar 2003 and Mitsubishi Lancer 1997) and four zenfone models mounted on four different racks were used in the experiment.

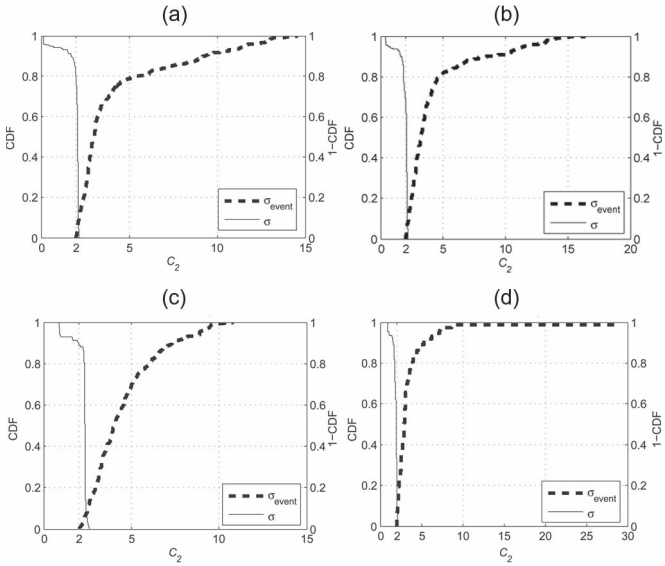

Fig. 8. Illustration of the selection of C_2. For each subplot, the dot line denotes the CDF of σ_{event}, and the solid line denotes the 1-CDF (survival function) of σ. The field test was performed in the same setting in Fig. 7.

B. Underdamped Oscillation Systems

The SPC is a complicated compound system of smartphones, vehicles, and even mounting racks. The vibrations of the mounted smartphone are affected by many facts, including the suspension systems of the vehicle, the mounting rack or adhering method, the weight of the smartphone, and even where the smartphone is located. Furthermore, the properties of the sensor, e.g., the sampling rate and accuracy level, are also concerns. To mitigate these factors on the vibrations of the mounted smartphone, we try to model the SPC system by the UOM [15].

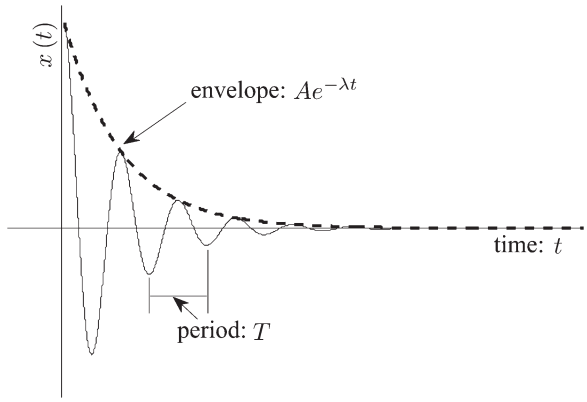

Fig. 9. Waveform of an underdamped oscillation.

TABLE I
UOM PARAMETERS FOR THE TOYOTA CAMRY 2013 FOUND BY THE NUMERICAL OPTIMIZATION AND THE CORRESPONDING RMSE OF THE MEASURED VACS TO THE NUMERICAL VALUES MODELED BY THE UOM WITH RESPECT TO DIFFERENT SPEED BUMPS

bumps	A	λ	ω	θ_0	RMSE
Bump1 (3.5 cm)	7.91	0.004	0.090	0.092	1.25
Bump2 (5 cm)	11.672	0.008	0.073	0.31	1.21

An underdamped oscillation system [15] is described by the differential equation

$$m\ddot{x} + b\dot{x} + kx = 0 \tag{4}$$

with $b^2 - 4mk < 0$, where x, m, b, and k are the position and mass of the object, the damping coefficient, and the spring coefficient, respectively. The solutions of the system are in the form of

$$\ddot{x}(t) = Ae^{-\lambda t}\cos(\omega t - \theta_0) \tag{5}$$

where $\omega = \sqrt{(k/m) - (b^2/4m^2)}$ is the angular frequency, $\lambda = b/2m$ is the distortion rate, θ_0 is the initial phase, and A is an amplitude parameter. θ_0 and A will be determined if initial conditions are given. A typical waveform of the acceleration of an underdamped system is illustrated in Fig. 9. In addition, the standard deviation of the acceleration from $t = t_0$ to $t = t_1$ can be calculated by

$$\sigma = A\sqrt{\frac{1}{t_1 - t_0}\left(\begin{array}{l}\int_{t_1}^{t_0}\left(e^{-\lambda t}\cos(\omega t - \theta_0)\right)^2 dt \\ -\left(\int_{t_1}^{t_0} e^{-\lambda t}\cos(\omega t - \theta_0)\, dt\right)^2\end{array}\right)}. \tag{6}$$

Investigating (6), we observe that the standard deviation is proportional to the initial amplitude parameter A and an integration of a function of cosine over the duration. For a given underdamped oscillation system, if we fixed the duration and always select the same θ_0, the square root part can be treated as a constant. Therefore, the standard deviation is only proportional to the amplitude. To index the bumping events, we propose to divide the standard deviation during the bumping periods by the standard deviation during the normal period. The

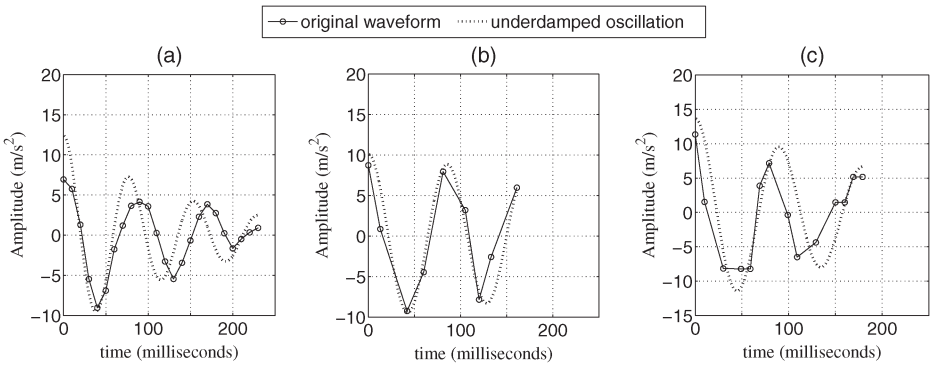

Fig. 10. Curve fits of the vibration waveforms and the underdamped oscillation waveforms for Toyota Camry 2013. (a) 3DM-GX3-25. (b) Padfone. (c) Sony Xperia S.

ratio can be a cross-SPC index on the road anomalies. Here, we implicitly assume that the bumping is positively related to the amplitude of the vibration. In the discretized version, the σ_i in the VCEH is an approximation of the standard deviation during the normal periods.

To validate whether the UOM is working or not, we performed two field tests in the NCTU campus. In the first test, a numerical optimization method was applied to find the parameters in the UOM. In the numerical optimization, we use the nonlinear optimization tool provided by MATLAB by solving the following minimization problem:

$$\min_{A,\lambda,\omega,\theta_0} \left(\sum_{i=1}^{N} \left(g_{t_i}^{\perp} - Ae^{-\lambda t_i} \cos(\omega t_i - \theta_0) \right)^2 \right)^{\frac{1}{2}} \quad (7)$$

where $g_{t_i}^{\perp}$ is the vertical acceleration component (VAC) at time t_i. The large-scale algorithm is used, which is based on the interior-reflective Newton method [16]. The search ranges for A, λ, ω, and θ_0 are $[-20, 20]$, $[0,1)$, $[0,1)$, and $[0, 2\pi]$, respectively; and the stepping size is determined by the trust region method. The optimization starts with a random guess and iteratively approximates the solution. For each iteration, it involves the approximate solution of a large linear system using the method of preconditioned conjugate gradients. In the experiment, four sensing devices, including three smartphones, i.e., two ASUS Padfone and one Sony Xperia S, and one accelerometer, i.e., 3DM-GX3-25, were used to collect vibration data. The sampling rates of Padfone, Xperia S, and 3DM-GX3-25 are 40, 80, and 100 Hz, respectively. Two speed bumps with heights of 3.5 and 5 cm were installed on the route. The smartphones and accelerometers were installed on two different kinds of racks. One Padfone and 3DM-GX3-25 were attached to the windshield, and the other Padfone and Sony Xperia S were attached to the back side window. Three vehicles, namely, Toyota Camry 2013, Toyota Camry 2010, and Lexus ES 2007, were used in the experiment. The vehicles were drove to run over the speed bumps at speeds about 20 and 40 km/hr, and five samples were recorded for each speed. In total, there were 240 samples collected (three vehicles, two speed bumps, four sensing devices, two speeds, and five samples).

Table I shows the UOM parameters found by the numerical optimization and the corresponding RMSEs of the measured VACs to the numerical values modeled by the UOM with respect to different speed bumps.[2] The parameters A, λ, ω, and θ_0 are calculated in average. The overall RMSEs for the speed bumps B1 and B2 are 1.25 and 1.21, respectively. Fig. 10 shows the curve fits of the vibration waveforms.

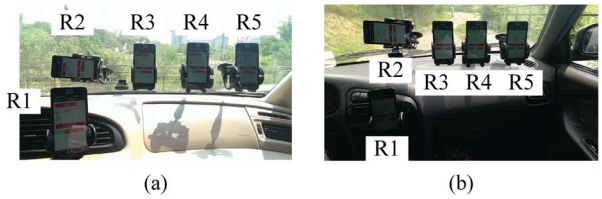

Fig. 11. Phone settings for (a) Ford Wind 2003 and (b) Mitsubishi Lancer 1997.

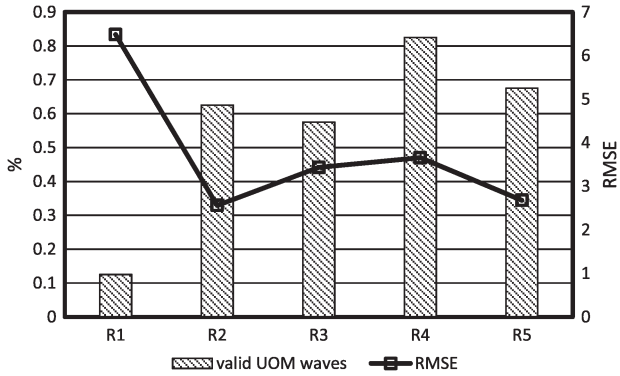

Fig. 12. Percentage of valid UOM waveforms and the corresponding RMSE for different phone racks.

In the second field test, the feasibility of UOM for various phone holders was tested. Two vehicles (Ford Windstar 2003 and Mitsubishi Lancer 1997), five zenfone models, and five different types of phone holders were used, as shown in Fig. 11. The vehicles were drove over two speed bumps each for ten times, and the caused vibrations were recorded by the detection application to see whether the vibration waveforms fit the UOM by checking the distortion rate λ and RMSE. If the distortion rate is found to be negative, it means that the waveform does not fit the UOM, and the RMSE is not taken into the statistic. Fig. 12 shows the percentage of valid UOM waveforms and

[2]Due to space limitations, the parameters and curve fits found for Toyota Camry 2013 are given here. For the details of the model verification and the RMSE analyses, please refer to [17].

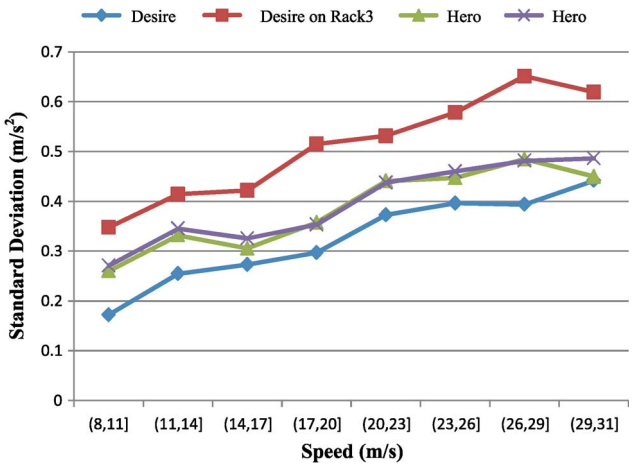

Fig. 13. Overall standard deviation at different speeds.

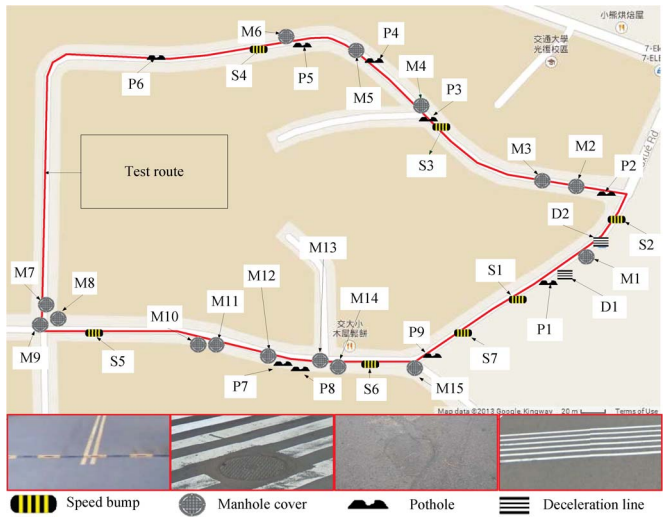

Fig. 14. NCTU campus scenario: There were seven speed bumps (S1–S7), 14 manhole covers (M1–M15), nine potholes (P1–P9), and two deceleration lines (D1 and D2) on the route.

the corresponding RMSE for different phone racks. The results show that racks attached to the air conditioner outlet (case in R1) was not fitted to the UOM.

C. Effects of Vehicle Velocity

Obviously, bump acceleration profiles of an anomaly are "bigger" if a vehicle drove over the same one but faster. The running speed of vehicles is another important factor affecting the vibration. To investigate the correlation of the vibration and speed, two experiments are conducted.

In the first experiment, two hTC Desire and two hTC Hero smartphones were used. All four smartphones were installed on a vehicle that was going to run on a highway on June 15, 2012. One hTC Desire was mounted on a rack labeled by $R3$, and the rest were attached to the windshield. The moving speeds were divided into eight ranges. The standard deviation σ of VCs of each smartphone in each speed range is illustrated in Fig. 13. The line marked with red squares is σ for hTC Desire mounted on rack R_3; and the lines marked with blue diamonds, green triangles, and purple crosses are σ' for the rest of the smartphones. We can observe that, in average, the vibration becomes more significant as the speed rises.

In the second experiment, two hTC Desire smartphones mounted on racks labeled by $R1$ and $R2$ were placed near the front seats and the rear seats of the same vehicle, respectively. The vehicle was driven at a speed between 10 and 30 km/hr along a cyclic route on NCTU campus on June 5, 2012, as illustrated in Fig. 14. Various road anomalies such as speed bumps, uneven manhole covers, and potholes are along the cyclic route. In total, five rounds of data collection were performed. Fig. 15 illustrates the measured σ_{event} due to the same anomaly. Since the two racks are of different types, they have various responses to the road anomalies. However, the similar trend is found that σ_{event} becomes larger as the vehicle runs faster. The trends of the two racks were calculated by linear regression and plotted in Fig. 15. Based on the results in the experiment, the parameters σ_{event} and σ_i should be grouped by speeds to reveal the speed effect on the vibration.

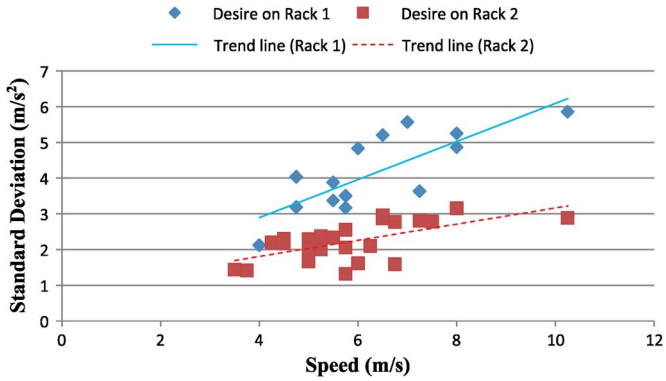

Fig. 15. Relation between σ_{event} and the vehicle speed in the NCTU campus scenario.

D. Indexing Anomalies

Although there exists a trend between the vibration magnitude and the vehicle speed, the evidence is not enough to build a model for the relation. Hence, we propose a lookup table approach to solve this issue. The speed is categorized into several ranges. The standard deviations of stable periods under different speed ranges are calculated separately. Let $\sigma(s)$ denote the standard deviation of stable periods of speed interval s. If the bumping event is detected at speed interval s, the AI of the event is included in the report and given by

$$AI = \frac{\sigma_{\text{event}}}{\sigma(s)}. \tag{8}$$

Recall the NCTU campus experiment. The speed domain is divided into ranges [4,7) and [7,10). Similarly, $(\sigma_{\text{event}}/\sigma, s)$ and $(\sigma_{\text{event}}/\sigma(s), s)$ are plotted in Fig. 16(a) and (b), respectively. In this case, the average AI of the speed bump is 10.23 with a standard deviation of 2.62. Similar phenomena can be found in the experiment. The slopes of the trend lines of R1 and R2 are 1.71 and 1.05 in Fig. 16(a) and 1.23 and 0.61 in Fig. 16(b), respectively.

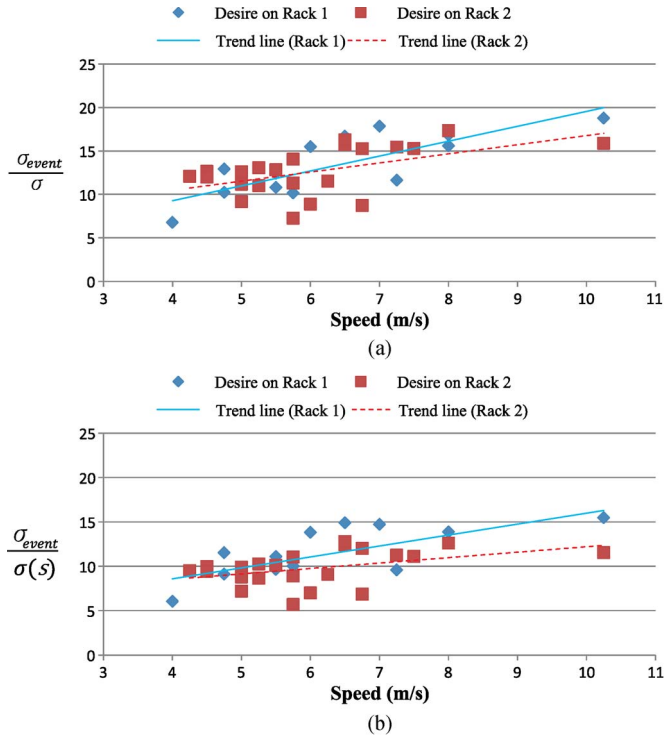

Fig. 16. AI for different speeds with respect to different racks. (a) AI derived by $\sigma_{\text{event}}/\sigma$. (b) AI derived by $\sigma_{\text{event}}/\sigma(s)$.

To further investigate factors that influence the vehicle vibrations, we further conduct a series of experiments. The factors controlled in the experiment include vehicle models, anomalies, phone racks, accelerometers, and driving speeds. The experiment setup is the same to the one introduced in Section V-B. Fig. 17 shows AIs with respect to the controlled factors. In the figure, C1, C2, and C3 denote Toyota Camry 2013, Toyota Camry 2010, and Lexus ES 2007, respectively. B1 and B2 denote bumps with heights of 3.5 and 5 cm, respectively. $Cx{-}By{-}S$ denote the AIs with respect to car Cx, bump By, and speed s. The AIs measured by 3DM-GX3-25 are used as the ground truth and represented by blue bars. The AIs measured by Padfone mounted on rack 1 (Padfone-R1), Padfone mounted on rack 2 (Padfone-R2), and Xperia S mounted on rack 2 (Sony-R2) are represented by red, green, and purple bars, respectively. It can be seen that AIs from the same bump under various setups were similar (in average, 3.33 for B1 and 4.57 for B2). Overall, the proposed AI can be a road anomaly assessment metric cross-SPC.

VI. System-Level Data Mining

Although the signal processing and road anomaly indexing provide device-level intelligence, the reported bumping events are still somewhat uncertain, such as false alerts, inaccurate indexing, and imprecise GPS position. Here, system-level data mining is applied to dig out comprehensive information. Experimentally, a grid-based clustering algorithm [18] called DENCLUE was adopted to demonstrate how to improve accuracy and retrieve information by system-level mining techniques. By applying DENCLUE, we may filter out false events based on the reporting frequency and improve the accuracy of position and index by averaging. In addition, the road anomaly information can be extended beyond the device level. For example, the hitting ratio of road anomalies, that is, the ratio of the number of reported events to the number of passing SPCs, may imply the type or dimension information; furthermore, by tracking the records of an anomaly, the appearance and repair of the anomaly can be learned. In the following, the version of DENCLUE used in the experiment is sketched.

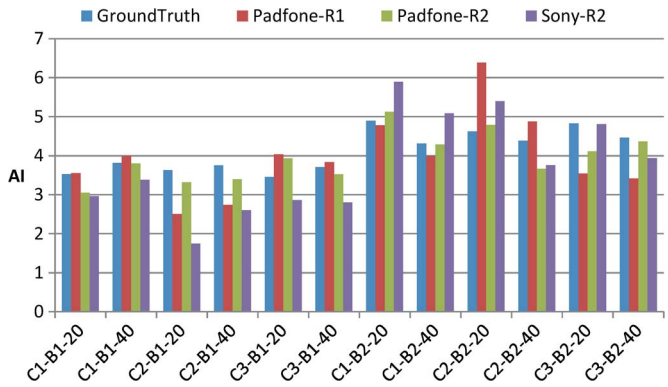

Fig. 17. AI with respect to controlled factors. The controlled factors include vehicle types, anomalies, sensing devices, phone racks, and speeds.

1) Divide the map into grids with equal grid size z. The density of a grid is defined as the frequency of anomalies in that grid. The grid size z is set to 5m in our implementation.
2) Find density attractors. A density attractor is defined as the grid with maximal density among its neighbor grids. Two grids are neighbors to each other if the distance between their centers is less than $\sqrt{2}z$. A cluster is formed for each density attractor. The neighbor grid of a density attractor is absorbed by that density attractor if the density of that neighbor grid is larger than or equal to a density threshold D. If the density of a grid is less than D, the grid is treated as noise. The density threshold D is set to 3 in our implementation.
3) Store the resulted cluster and related information to the database. The resulted clusters represent distinguishable anomalies, and the location and index information of the anomaly are determined by averaging the location and AI in the cluster, respectively.

A. NCTU Campus Scenario

The NCTU campus scenario introduced in Section V-C is investigated. Two smartphones were installed on the vehicle, and five rounds of experiments were executed. The GPS sampling rate is set to 1 Hz. The sampling rate for the hTC Hero model is 46 Hz. The results before and after clustering are depicted in Fig. 18. The gray and purple balloons represent reported and clustered events, respectively. The results show that most anomalies were detected, e.g., the speed bumps are all detected, but some anomalies such as manhole covers, deceleration lines,

Fig. 18. Results of anomaly detection in the NCTU campus scenario. The gray balloons represent the events detected by the bumping detection algorithm, and the purple balloons represent the events after clustering.

TABLE II
POSITION ACCURACY AND AI OF DIFFERENT ROAD ANOMALIES INCLUDING THE SPEED BUMP, THE MANHOLE COVER, THE DECELERATION LINE, AND THE POTHOLE

type of anomalies	accuracy (mean/stdev)	AI (mean/stdev)
speed bump	$7.5m/2.5m$	$5.83/0.30$
manhole cover	$6.0m/2.3m$	$4.23/0.38$
deceleration line	$6.1m/2.5m$	$4.90/0.7$
pohole	$5.3m/2.1m$	$4.60/0.30$

and potholes are not detected. This is because some potholes and manhole covers did not necessarily get hit in each round, but speed bumps usually did. Since the digital maps provided by Google Maps services have offsets to the real maps, it should be noted that the detected events have position errors while showing in the Google Maps. In addition, since some anomalies are very close to each other, they may be treated as the same one by the clustering algorithm. To further investigate the accuracy and indexing after clustering, we do statistic on the hitting ratio, accuracy of positioning, and AI for different anomalies. However, due to space limitations, we present the average and standard deviation of positioning accuracy and AI here. The positioning accuracy and AI of the speed bump, the manhole cover, the deceleration line, and the pothole are shown in Table II. Through the above experimental results, possible benefits from the system-level intelligence could be envisioned.

VII. CONCLUSION

In this paper, SPCs have been deployed as crowdsources to pervasively and continuously monitor road conditions by mobile sensing technologies. For road pavement monitoring, we developed an SPC system that provides the capacity to detect and index run-over road anomalies. For mass deployment and supporting to subsequent system-level data mining, the proposed system has two advantages in the device level. First, it is an adaptive and driver-friendly system. No complicated installation and no training processes are needed. Drivers only need to mount the smartphone firmly on their vehicles. Second, the system provides an SPC-independent road anomaly indexing mechanism. The assessment can provide similar indices for the same road anomaly even by different SPCs at different vehicle speeds. In addition, a grid-based clustering is used to demonstrate the benefit of improving detection accuracy in the system level. However, many issues are not covered in this paper. For example, this paper discusses the road surface assessment in the time domain; however, the road maintenance community usually makes long-term decisions about larger areas, i.e., in the distance domain. The relationship between the AI and other roughness indexes such as IRI and quality index is other possible future research direction. In addition, the self-adaptive mechanism to select the best parameters that adapt to the environment is an important issue. A road management system is needed to provide a system-level statistics such as road quality ranking and quality assessment on maintenance units. These issues deserve further efforts in the future.

REFERENCES

[1] K. D. Zoysa, C. Keppitiyagama, G. P. Seneviratne, and W. W. A. T. Shihan, "A public transport system based sensor network for road surface condition monitoring," in *Proc. ACM SIGCOMM Workshop NSDR*, 27 Aug. 2007, pp. 1–6.
[2] J. Eriksson *et al.*, "The pothole patrol: Using a mobile sensor network for road surface monitoring," in *Proc. 6th Int. Conf. MobiSys*, Jun. 17–20, 2008, pp. 29–39.
[3] P. Mohan, V. N. Padmanabhan, and R. Ramjee, "Nericell: Rich monitoring of road and traffic conditions using mobile smartphones," in *Proc. 6th Int. Conf. Embedded Netw. Sensys.*, Nov. 5–7, 2008, pp. 357–358.
[4] Y.-C. Tai, C.-W. Chan, and J. Y.-J. Hsu, "Automatic road anomaly detection using smart mobile device," in *Proc. Conf. TAAI*, Nov. 18–20, 2010, pp. 1–8.
[5] A. Mednis, G. Strazdins, R. Zviedris, G. Kanonirs, and L. Selavo, "Real time pothole detection using android smartphones with accelerometers," in *Proc. Int. Conf. DCOSS*, Jun. 27–29, 2011, pp. 1–6.
[6] J. Dawkins, R. Bishop, B. Powell, and D. Bevly, "Investigation of pavement maintenance applications of intellidrive^{SM} (Final Report): Implementation and deployment factors for vehicle Probe-based Pavement Maintenance (PBPM)," Auburn Univ., Auburn, AL, USA, May 2011.
[7] Street Bump project. [Online]. Available: http://www.streetbump.org/
[8] M. Ndoye, A. M. Barker, J. V. Krogmeier, and D. M. Bullock, "A recursive multi-scale correlation-averaging algorithm for an automated distributed road condition monitoring system," *IEEE Trans. Intell. Transp. Syst.*, vol. 12, no. 3, pp. 795–808, Sep. 2011.
[9] A. Mednis, A. Elsts, and L. Selavo, "Embedded solution for road condition monitoring using vehicular sensor networks," in *Proc. 6th Int. Conf. AICT*, 2012, pp. 1–5.
[10] R. Labayrade, D. Aubert, and J.-P. Tarel, "Real time obstacle detection in stereovision on non flat road geometry through 'v-disparity' representation," in *Proc. IEEE Intell. Veh. Symp.*, 2002, vol. 2, pp. 646–651.
[11] J. Han, D. Kim, M. Lee, and M. Sunwoo, "Enhanced road boundary and obstacle detection using a downward-locking lidar sensor," *IEEE Trans. Veh. Technol.*, vol. 61, no. 3, pp. 971–985, Mar. 2012.
[12] The Flatness of Roads Project Report (in Chinese). Taipei Government, vol. 10, no. 7, Apr. 2010.
[13] M. W. Sayers, "On the calculation of international roughness index from longitudinal road profile," *Transp. Res. Rec.*, no. 1501, pp. 1–12, 1995.
[14] Google Maps API. [Online]. Available: https://developers.google.com/maps/
[15] C. W. de Silva, *Vibration Damping, Control, and Design*, Boca Raton, FL, USA: CRC Press, Apr. 2007.
[16] T. F. Coleman and Y. Li, "An interior trust region approach for nonlinear minimization subject to bounds," *Soc. Ind. Appl. Math.*, vol. 6, no. 2, pp. 418–445, May 1996.
[17] Y.-T. Chuang, C.-W. Yi, T.-H. Wu, and C.-Y. Chan, "Model the vibrations of rack-mounted on-vehicle devices by underdamped oscillations," in *Proc. 17th ITSC*, Oct. 8–11, 2014, pp. 982–987.
[18] A. Hinneburg and D. A. Keim, "An efficient approach to clustering in large multimedia databases with noise," in *Proc. 4th Int. Conf. KDD*, Aug. 27–31, 1998, pp. 58–65, AAAI Press.

Chih-Wei Yi (M'13) received the B.S. and M.S. degrees from National Taiwan University, Taipei, Taiwan, and the Ph.D. degree from Illinois Institute of Technology, Chicago, IL, USA.

He was a Senior Research Fellow with the Department of Computer Science, City University of Hong Kong, Hong Kong. He is currently an Associate Professor of computer science with National Chiao Tung University, Hsinchu, Taiwan. His research focuses on wireless ad hoc and sensor networks, vehicular ad hoc networks, network coding, and algorithm design and analysis.

Dr. Yi is a member of the Association for Computing Machinery. He received of the Outstanding Young Engineer Award from the Chinese Institute of Engineers in 2009.

Yi-Ta Chuang is currently working toward the Ph.D. degree in computer science at National Chiao Tung University, Hsinchu, Taiwan.

His research interests are in mobile sensing, wireless ad hoc networks, vehicular ad hoc networks, and applications of telematics.

Chia-Sheng Nian received the Master's degree in computer science from National Chiao Tung University, Hsinchu, Taiwan.

He is with HTC Corporation, Taipei, Taiwan. His research interests include vehicular ad hoc networks and applications of telematics.